Vibrational Assignment of Energetic Material 5-Nitro-2,4-dihydro-1,2,4-triazole-3-one (NTO) with Labeled Isomers

Reiko I. Hiyoshi,*,† Yuji Kohno,*,‡ and Jun Nakamura†

Explosion Investigation Section, National Research Institute of Police Science, Kashiwanoha 6-3-1, Kashiwa, Chiba 277-0882, Japan, and Interdisciplinary Shock Wave Research Laboratory, Institute of Fluid Science, Tohoku University, Katahira 2-1-1, Aoba-ku, Sendai 980-8577, Japan

Received: February 27, 2004; In Final Form: April 19, 2004

The Infrared (IR) and Raman spectra of 5-nitro-2,4-dihydro-1,2,4-triazole-3-one (NTO) and its compounds labeled with the stable isotopes ^{15}N, ^{13}C, and deuterium (D) (such as NTO-$^{15}NO_2$, NTO-$^{13}C(3)$ or NTO-D) were measured in the region of 100−3500 cm^{-1}. Vibrational motions were experimentally assigned by using isotopic vibrational shifts. In addition, theoretical calculations were performed to assign those vibrational bands with good agreement of experimental and theoretical data. Furthermore, the experimental and calculated results indicate that the C−O bond length of NTO in the crystal state is longer than that of an isolated molecule in the gas phase because of intermolecular hydrogen bonding.

1. Introduction

5-Nitro-2,4-dihydro-1,2,4-triazole-3-one (NTO) is well-known as an insensitive explosive, and there are many reports about its decomposition process,[1−4] explosion properties such as sensitivity and detonation velocity,[5−7] crystalline structure,[8−10] and computational chemistry.[11−18] Vibrational spectra of NTO are given in some papers, but there is no report about experimental vibrational assignment. To investigate the chemical structural change of NTO with vibrational spectra under high pressure, i.e., static pressure in Diamond Anvil Cell (DAC) or dynamic pressure such as shock wave propagation, it is necessary to clearly assign the IR and Raman bands. The proper assignments will also help to evaluate chemical properties of NTO. In this work, some of the labeled compounds of NTO were prepared with stable isotope-labeled starting materials such as urea-^{13}C, and vibrational assignments were performed by using isotopic shifts and theoretical calculations.

2. Experimental Section

(1) Preparation of Labeled NTO. Labeled NTOs were synthesized by the method of Oxley[19] with some modifications. All of the labeled products are shown in Figure 1. Starting materials for isotope labeling were urea-^{13}C (NTO-$^{13}C(3)$), urea-$^{15}N_2$ (NTO-$^{15}N(4)$), potassium nitrate-^{15}N (NTO-$^{15}NO_2$), and hydrazine sulfate-$^{15}N_2$ (NTO-$^{15}N(1,2)$). Products were purified by recrystallization from water (H_2O). NTO-D_2 was obtained by recrystallization of normal NTO from heavy water (D_2O). The purity and the production of labeled NTOs were confirmed with high performance liquid chromatography (Hewlett-Packard, LC1100) and mass spectrometry (Shimadzu, QP5000).

(2) Vibrational Spectroscopy. IR spectra were obtained by the attenuated total reflection (ATR) method with a Fourier transform infrared spectrometer (Thermo Electron Co., Nicolet Nexus 670) in the range of 650−3500 cm^{-1} with a resolution of 1 cm^{-1} for all spectra. Samples were lightly ground in preparation for placement on the ATR stage. Raman spectra were measured (Thermo Electron Co., Nicolet Almega) in the range of 100−3500 cm^{-1} with a laser wavelength of 532 nm (laser power: ∼1 mW) and a resolution of 2−5 cm^{-1}. Samples were held on a glass slide in their normal crystalline condition.

All of the measurements were taken at room temperature (around 20 °C).

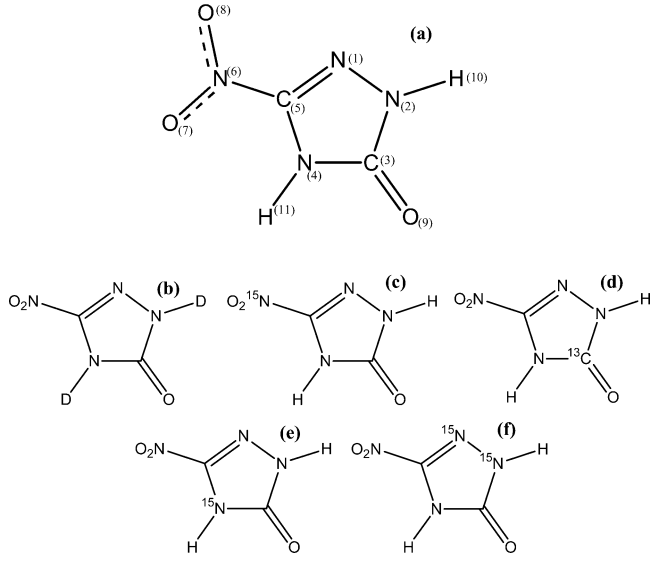

Figure 1. Labeled NTOs: (a) NTO-normal, (b) NTO-D_2, (c) NTO-$^{15}NO_2$, (d) NTO-$^{13}C(3)$, (e) NTO-$^{15}N(4)$, (f) NTO-$^{15}N(1,2)$.

(3) Computational Method. *Ab initio* calculations were carried out with the GAUSSIAN-98[20] program package. The basis sets implemented in the program were employed without modification. The geometry of NTO was fully optimized without symmetry constraints by the energy gradient methods. All optimized geometries were obtained by using the HF (Hartree−Fock), MP2 (second-order Mϕller−Plesset perturbation), and Becke 3LYP(B3LYP) hybrid density functional with the

* Address correspondence to these authors. R.I.H.: phone +81-4-7135-8001, fax +81-4-7133-9169, e-mail ichiki@nrips.go.jp. Y. K.: phone +81-22-217-5285, fax +81-22-217-5324, e-mail kohno@rainbow.ifs.tohoku.ac.jp.
† National Research Institute of Police Science.
‡ Institute of Fluid Science.

10.1021/jp049118i CCC: $27.50
Published on Web 06/11/2004

TABLE 1: Wavenumber Shifts of Isotopic Labeled NTOs[a]

normal		$^{13}C{=}O$		$^{15}NO_2$		$^{15}N(4)$		$^{15}N(1,2)$		D_2	
Raman	IR	Raman	IR	Raman	IR	Raman	IR	Raman	IR	Raman	IR
146		145		145		146		142		144	
		188									
192		192		192		189		192		188	
227		226		227		226		225		224	
		241									
243		245		243		242		242		241	
								337 sh			
347		346		346		345		340		345	
418		416		416		418		416		416	
473		469		472		470		471		465	
585		583		584		583		581		584 w	
600		600		597		598		593		620	
691	682	691	681	686	680	691	679	692	679	687	684
	723		710	717 sh	718	721 sh	723	720 sh	723		722
729	731	715	733	724	726	728		728	728	733	731
742 sh	750 sh					741 sh			749		748
751	755	748	750	749	750	750	750 sh	745	742 sh	752 w	753
					757 sh		754				
	762 sh	755 sh	755	758 sh	759 sh	758 sh	761	753 sh		760	757
	787		782		786		784		785		784 w
										815	814
830	829	830	828	824	823	831	829	828	825	830	829 w
	948		945				941		932		
1009 sh	1006	1010 sh	1004	1009 sh	1006	1005 sh	993	996 sh	994		997
										999	1005 sh
1018	1018	1018	1016	1018	1017	1001	1004	1005	1004	1017	1016 w
		1095					1101				
1104	1109	1102	1095	1104	1111	1102	1108	1084	1088	1104	1108
1190	1188	1187	1184	1190	1188	1187	1185	1188	1185		1188
1255		1253		1245		1253		1250			
1286	1280	1265	1261	1287	1282	1281	1274	1272	1267	1267	1267
1332	1340	1330	1338	1334	1329	1332	1336	1321	1336	1338	1333
1360	1355 sh	1360	1351	1334	1360 sh	1357	1351 sh	1358	1354	1358	1354
		1417									
		1434	1427								
1475	1473	1474	1471	1472	1471	1464	1459	1476	1474	1453	1450
1545	1541	1544	1540	1514	1511	1545	1541	1544	1539	1544	1540
1548 sh	1546 sh	1548 sh	1545 sh	1518 sh	1516	1548 sh	1545 sh				
1593	1590 vw	1592	1589	1590	1590	1592 sh		1576 sh	1590	1589	1588
1599 sh	1600	1596 sh		1594 sh	1594	1596	1596	1586			
	1674 sh		1639		1674 sh		1672 sh		1670 sh		1659 sh
1702	1691	1657	1652 sh	1702	1693	1701	1690	1701	1692	1699	1692
	1712		1726 vw		1714		1711 sh		1709 sh		
3192	3198	3192	3194	3194	3201	3197	3197	3184	3184	2389	3201
3241	3242	3242	3239	3243	3242	3235	3238	3243	3244	2437	3249

[a] sh = shoulder, w = weak, vw = very weak; all frequencies are in cm^{-1}.

6-311++G(2df,2dp) (split-valence plus diffuse functions plus 2df polarization functions on heavy atoms and 2dp polarization functions on the hydrogen atoms basis set). Vibrational frequencies were calculated by using the analytical second derivatives at the HF/6-311++G(2df,2dp), the MP2(Full)/6-311++G(2df,-2dp), and the B3LYP/6-311++G(2df,2dp) levels to confirm the stationary structures and to correct for the zero-point vibrational energy. The values of harmonic vibrational frequencies determined at various levels have been scaled by 0.8929 at HF/6-311++G(2df,2dp), 0.9427 at MP2(Full)/6-311++G(2df,2dp), and 0.9613 at B3LYP/6-311++G(2df,2dp) levels.[21]

3. Result and Discussion

(1) Experimental Assignment of IR and Raman Bands with NTO Isomers. NTO exists in two polymorphic forms known as α and β. The α form is stable at room temperature and is used in the general applications. The α form is well-known as a twinned crystal, and it is usually obtained from common recrystallization where as the β form is only recrystallized with a special treatment.[8] In this work, all of obtained crystal form is α-NTO. Because of this interesting physical property of crystal twinning, there is a dependence of Raman intensity on the orientation of the crystal reported by Franken et al.[22] However, in this work, only largely grown α-NTO crystals were used for Raman measurement and it was supposed that the crystal faced the same plane to the laser beam in each measurement. While our measurement conditions were different than those of Franken, one of their spectrum intensity patterns, facing the (100) plane to the laser beam, was similar to ours. There were no deviations of wavenumbers due to the crystal orientation in our spectra and assignments did not pose any problems. The IR and Raman spectra are shown in Figure 2 in full range.

The IR and Raman spectra of the NTO isomers are shown in Figures 3−5. Intensity and frequency corrections were made to all of the ATR-IR spectra. There has been a change of relative intensity of IR and Raman bands in some isotopic labeled compounds for some reason, this, however, did not interfere

TABLE 2: Geometrical Parameters of NTO Molecule

	geometrical parameter				
	theoretical			experimental[b]	
structural parameter	HF/6-311++G (2df,2pd)	MP2/6-311++G (2df,2pd)	B3LYP/6-311++G (2df,2pd)	Lee et al.[8,13]	Zhurova et al.[10]
r(N1−N2)	1.352	1.356	1.357	1.369(2)	1.3658(3)
r(N2−C3)	1.366	1.386	1.394	1.367(2)	1.3737(3)
r(C3−N4)	1.379	1.397	1.400	1.378(2)	1.3795(3)
r(N4−C5)	1.356	1.351	1.362	1.349(2)	1.3556(4)
r(C5−N1)	1.252	1.301	1.288	1.290(2)	1.2987(4)
r(N2−H10)	0.990	1.005	1.005	0.875[13]	1.0090(2)
r(C3−O9)	1.183	1.207	1.203	1.226(2)	1.2343(3)
r(N4−H11)	0.991	1.006	1.006	0.916[13]	1.0090(2)
r(C5−N6)	1.444	1.434	1.447	1.447(2)	1.4430(4)
r(N6−O7)	1.173	1.221	1.213	1.217(2)	1.2253(3)
r(N6−O8)	1.188	1.232	1.228	1.218(2)	1.2279(3)
θ(N1−N2−C3)	113.6	115.2	114.3	112.8(1)	112.6[a]
θ(N2−C3−N4)	114.1	113.9	113.7	103.8(1)	114.6[a]
θ(C5−N1−N2)	103.8	102.4	103.5	102.4(1)	102.9[a]
θ(H10−N2−N1)	120.4	119.6	120.2	115.7[13]	120.1[a]
θ(O9−C3−N2)	129.3	129.8	129.4	126.9(1)	126.7[a]
θ(O9−C3−N4)	128.9	129.6	129.8	129.3(1)	129.3[a]
θ(H10−N2−C3)	126.0	125.1	125.5	123.3[13]	127.4[a]
θ(N6−C5−N4)	121.6	121.8	122.0	123.2(1)	123.2[a]
θ(O7−N6−C5)	118.1	118.1	118.4	116.2(1)	116.5[a]
θ(O8−N6−C5)	114.7	114.7	114.7	117.4(1)	117.4[a]
θ(O7−N6−O8)	127.3	127.2	126.8	126.4(2)	126.1[a]
τ(N1−N2−C3−N4)	0.0	0.0	0.0	0.06[13]	0.00[a]
τ(C5−N1−N2−C3)	0.0	0.0	0.0	0.44[13]	0.00[a]
τ(N6−C5−N1−N2)	180.0	180.0	180.0	178.92[13]	178.50[a]
τ(O7−N6−C5−N1)	0.0	0.0	0.0	−3.33[13]	177.40[a]
τ(O8−N6−C5−N4)	0.0	0.0	0.0	−2.53[13]	176.10[a]

[a] Calculated by using the atomic position.[10] [b] Values in parentheses are estimated standard deviations. Bond lengths are in angstroms and angles are in degrees.

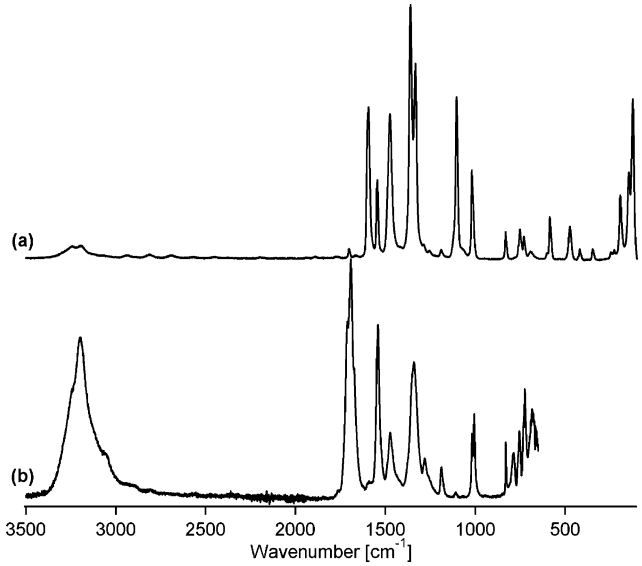

Figure 2. IR and Raman spectra of NTO: (a) Raman, laser 532 nm (∼1 mW), resolution 2−5 cm^{-1}; (b) IR, resolution 1 cm^{-1}.

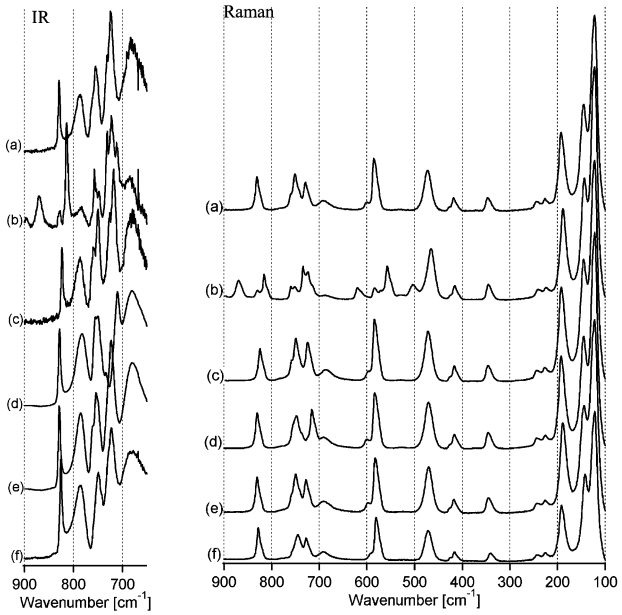

Figure 3. IR and Raman spectra of NTO isomers in the low wavenumber region: (a) NTO-normal, (b) NTO-D_2, (c) NTO-$^{15}NO_2$, (d) NTO-$^{13}C(3)$, (e) NTO-$^{15}N(4)$, (f) NTO-$^{15}N(1,2)$.

with this study. Particular shifts are observed in labeled compounds to normal NTO. Vibrational shifts are listed in Table 1. Assignment of NTO vibrations with only experimental data was very difficult because vibrational motions couple in various patterns, and therefore the shifting with labeled compounds was complicated. Especially, the isomer labeled with deuterium (D) usually shows large shifts and separation of vibrational couplings. However, there are some prominent wavenumber shifts on $-NO_2$ and >C═O with NTO-$^{15}NO_2$ and NTO-$^{13}C(3)$ isomers, respectively.

The Raman band 1545 cm^{-1} (shoulder: 1548 cm^{-1}) and IR band at 1541 cm^{-1} (shoulder: 1546 cm^{-1}) of normal NTO in Figure 4 showed red shifts with NTO-$^{15}NO_2$ where there were no (or slight) changes with other labeled isomers on the spectra. Those were experimentally assigned as $-NO_2$ asymmetric stretching because of the wavenumber and relative intensity of the IR and Raman bands.

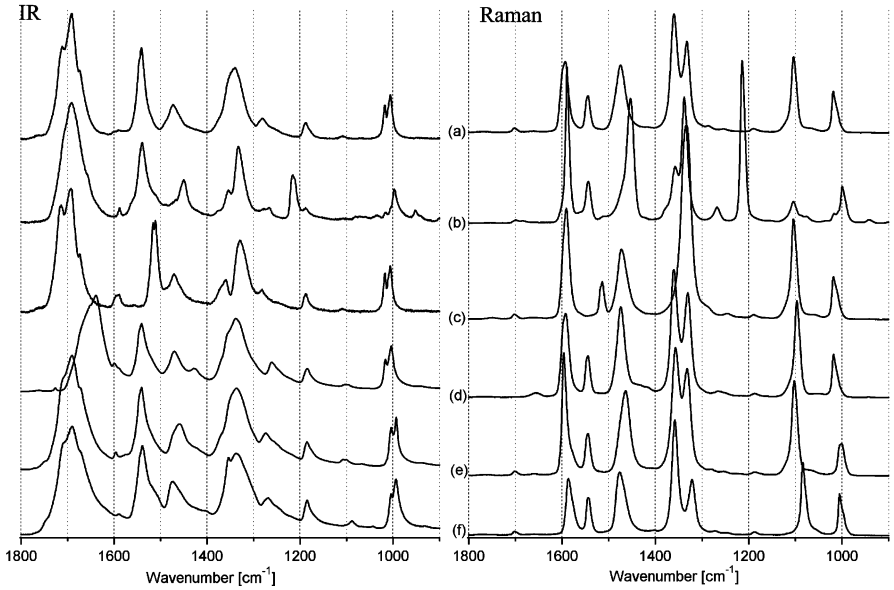

Figure 4. IR and Raman spectra of NTO isomers in the fingerprint region: (a) NTO-normal, (b) NTO-D_2, (c) NTO-$^{15}NO_2$, (d) NTO-$^{13}C(3)$, (e) NTO-$^{15}N(4)$, (f) NTO-$^{15}N(1,2)$.

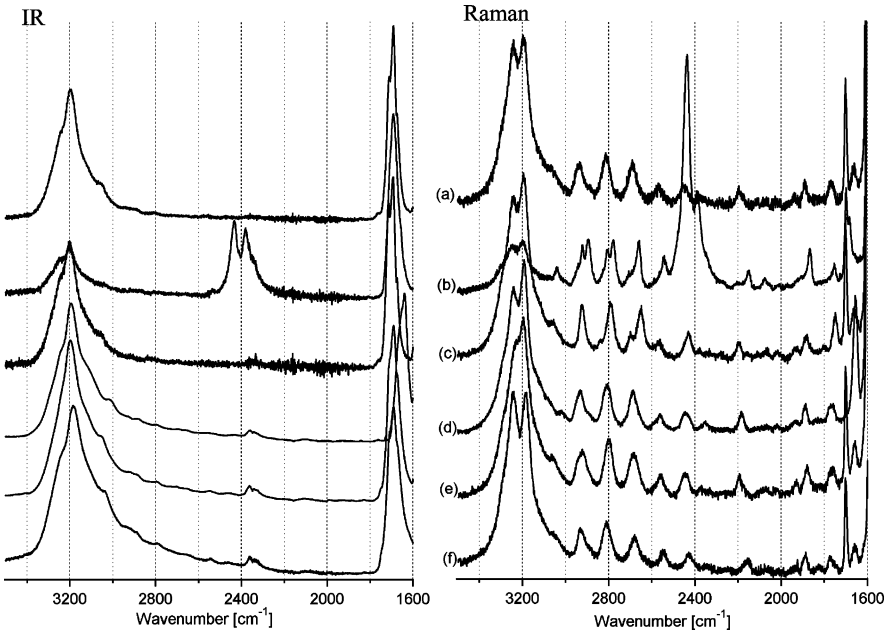

Figure 5. IR and Raman spectra of NTO isomers in the high wavenumber region: (a) NTO-normal, (b) NTO-D_2, (c) NTO-$^{15}NO_2$, (d) NTO-$^{13}C(3)$, (e) NTO-$^{15}N(4)$, (f) NTO-$^{15}N(1,2)$.

The Raman band at 830 cm^{-1} and IR band at 829 cm^{-1} in Figure 3 had small red shifts with NTO-$^{15}NO_2$. These are assumed as the $-NO_2$ deformation due to the wavenumber region. There is a slight effect with NTO-$^{15}N(1,2)$, which implies this band is also influenced by ring deformation.

The doublet Raman band 1332, 1359 cm^{-1} and IR band 1340 cm^{-1}(shoulder: 1355 cm^{-1}) in Figure 4 show red shifts with NTO-$^{15}NO_2$ as well, which are most likely related to $-NO_2$ symmetric stretching. Additionally, this vibration seems to be coupled with ring vibration because of slight shifts with ^{13}C-(3), $^{15}N(1,2)$, and $^{15}N(4)$ isomers.

The Raman band at 1702 cm^{-1} shifted to 1657 cm^{-1} only with NTO-$^{13}C(3)$ as shown in Figure 5. In the IR spectra (Figure 4), there are some other bands in this region and it was difficult to find out which particular wavenumber had shifted, but only NTO-$^{13}C(3)$ shows a considerable change. This red shift implies that those bands are related to the carbonyl group (>C═O).

Vibrations in the region of 1000−1300 cm^{-1} (Figure 4) are related to ring deformation, which had small red shifts with all labeled compounds except NTO-$^{15}NO_2$ as listed in Table 1. It is plausible to assign these bands as ring vibrations in this region.

The vibrational assignments of NTO based on theoretical calculations had been reported by several research groups.[11−18] In the result of Sorescu et al.,[13] there is good agreement in their scaled frequencies determined at B3LYP/6-311G**, B3LYP/6-311++G**, and MP2/6-311G** levels. In their result, however, the $-NO_2$ vibration frequency by DFT (1584.2 cm^{-1}) did not agree with the value calculated by MP2 (1723.1 cm^{-1}). They mentioned that the origin of this large deviation was not clear. Prabhakaran et al.[23] conducted comparisons of similar molecules to NTO such as the methyl derivative compound or urea, but they could not explain some unusual wavenumbers for some particular functional group vibrations in NTO. In contrast to their conclusion, there is no uncertainty for the

TABLE 3: Theoretical and Exprimental Vibrational Frequencies and Assignment[a]

	scaled theoretical vibrational freq			exptl vibrational freq				
				IR		Raman	IR	
mode	HF/ 6-311++G (2df,2pd)	MP2/ 6-311++G (2df,2pd)	B3LYP/ 6-311++G (2df,2pd)	thin film[13]	Ar matrix[13]	this work crystal	this work crystal	assignment
1	69.8	74.6	80.6			122		ring-NO_2 def out of plane
2	140.7	141.9	138.8			192		ring def + ring-NO_2 def out of plane
3	200.8	192.6	194.8			277/243		ring-NO_2 def in plane
4	287.0	293.7	294.7			347		ring def + ring-NO_2 def out of plane
5	400.7	389.0	389.8			418		C−NO_2 str + C−O def + NO_2 def in plane
6	430.8	441.5	445.8			427		NO_2 def + ring-NO_2 def + C−O def in plane
7	457.6	480.8	470.6	480	512	473		N−H def + ring def out of plane
8	497.7	537.0	521.8		573	585		N−H def + ring def out of plane
9	572.2	548.7	559.4	606	613	600		ring-NO_2 def + C−O def in plane
10	638.4	621.7	632.4	693		691	682	ring def out of plane
11	736.4	707.3	717.0	728	730	729	731	ring def out of plane
12	761.8	707.7	723.8	751	738	751	750	ring def + NO_2 def in plane
13	811.3	732.5	752.0	805			787	ring def + ring-NO_2 def out of plane
14	844.8	787.1	807.4	830	822	830	829	ring def + NO_2 def in plane
15	962.0	938.8	944.5		991	1009	1006	ring def + N−H def in plane
16	984.3	952.7	970.2	1021		1018	1018	ring def + N−H def + ring-NO_2 str in plane
17	1084.0	1086.6	1043.2	1111	1085	1104	1109	ring def (N1−N2−C3 asym str) in plane
18	1184.8	1133.6	1160.2	1185	1174	1190	1188	ring def + N−H def in plane
19	1262.6	1205.9	1217.0	1282	1257	1286	1280	ring def (N1−N2−C3 sym str + N2−C3−N4 asym str) + N−H def in plane
20	1372.0	1289.5	1313.2		1361	1360	1355	NO_2 def + NO_2 sym str + N−H def in plane
21	1405.6	1313.1	1335.8	1343	1338	1332	1340	N−H def + ring def (N1−N2−C3 asym str) in plane
22	1480.4	1424.7	1409.2	1477	1463	1475	1473	ring def (N4−C5 str) + N−H def + NO_2 def in plane
23	1638.3	1496.8	1534.7			1545	1541	ring def (N1−C5−N4) + N−H def + NO_2 asym str in plane
24	1673.5	1671.8	1562.4	1550	1563	1548	1546	ring def (N1−C5−N4) + ring-NO_2 def + N−H def + NO_2 asym str in plane
						1593	1590	related to N−N2 (Raman active)
				1605		1599	1600	
25				1695	1768		1691	C═O str
	1776.4	1748.6	1768.6	1716	1789	1702	1712	
26	3478.6	3483.9	3517.6	3200	3489	3192	3198	N(2)−H str
27	3493.4	3491.1	3518.4			3241	3242	N(4)−H str

[a] def = deformation, str = stretching, sym = symmetric, asym = asymmetric; all frequencies are in cm^{-1}.

assignment with our experimental data. At least assignments for −NO_2 and >C═O vibrations were experimentally determined. All of vibrational shifts with correlations of labeled isomers are listed in Table 1.

(2) Theoretical Data and Assignment of Vibrations. First of all, we carried out a full geometry optimization for the isolated NTO molecule in comparison with the experimental values as shown in Table 2. As seen by comparing the experimental data to the theoretical results at HF/6-311++G-(2df,2pd), MP2(Full)/6-311++G(2df,2pd), and B3LYP/6-311++G(2df,2pd) levels, the optimized bond lengths are in good agreement with experimental values[10] of the crystalline state. However, there is a little difference in the C−O bond length. The calculated C−O distance, 1.183−1.207 Å, is smaller than the corresponding experimental distance in the crystalline state (1.2343(3) Å). The difference is about 0.05−0.03 Å, and such shortening occurs only on the C−O bond. The crystalline structure of NTO shows that the C−O oxygen forms a hydrogen bond with the hydrogen of the N−H group of the other NTO molecule. These results indicate that there is an intermolecular effect (hydrogen bonding) especially shown on the C−O bond length of NTO in the crystalline state that is longer than the optimized value in the gas phase.

Ab initio calculated and experimental vibrational frequencies of NTO and assignments are listed in Table 3. All assignments were determined by comparison of experimental shifted data of the labeled NTOs with the calculated wavenumbers and vibrational motions at each mode. The calculated IR spectrum at the B3LYP/6-311++G(2df,2pd) level is presented with

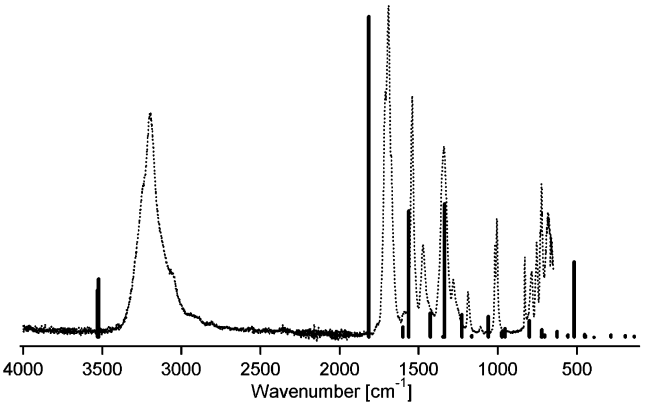

Figure 6. Theoretical and experimental IR spectra of NTO: solid line, theoretical; dashed line, experimental.

experimental data in Figure 6. There are some differences of wavenumbers between calculated and experimental data. This is because the calculated spectrum corresponds to the gas phase where experimental data are taken with solid NTO. However, these spectrum patterns are similar.

In the previous section, assignments for −NO_2 and >C═O vibrations were discussed. Therefore, these experimental wavenumbers of −NO_2 and >C═O vibrations can be compared to the calculated values. There are good agreements on modes 23 and 24, both of which are assigned as the −NO_2 asymmetric stretching in plane; the observed values of IR are 1541 and 1546 cm^{-1} at the shoulder compared to 1534.7 and 1562.4 cm^{-1}

calculated at the B3LYP/6-311++G(2df,2pd) level as shown in Table 3. This difference is due to the fact that the measurement takes place in the solid state, while the calculation is for the gas phase, i.e., isolated molecule. For instance, in the gas phase, mode 24 shows up to 1563 cm^{-1}. On the other hand, there is a poor agreement for the $-NO_2$ asymmetric vibration on the calculation levels of HF/6-311++G(2df,2pd) (1673.5 cm^{-1}) and MP2/6-311++G(2df,2pd) (1671.8 cm^{-1}).

For mode 25, the experimental IR band (1691 cm^{-1}) assigned as >C═O stretching is smaller than our three types of calculated values (1776.4, 1749.9, and 1768.6 cm^{-1}). As stated above, these calculated values correspond to the experimental wavenumber in the gas phase (1768 cm^{-1}). Expectedly, it was found that there is a difference of wavenumbers between the gas and crystalline phases, which can be linked with the results mentioned in the previous discussion regarding bond length. When the C−O bond forms a hydrogen bonding to the N−H group of the other NTO, the optimized C−O distance (1.183−1.207 Å) is smaller than the corresponding distance in the crystalline state (1.2343(3) Å). There is no contradiction to the result that the wavenumber of >C═O stretching in the crystalline state may be a smaller value compared to the gas phase (i.e., the optimized value).

(3) Deformation of the NTO Molecule. As described in the previous sections, interesting deformation patterns are observed in crystalline NTO, compared to the molecule in the gas phase.

The most important and prominent difference is hydrogen bonding. Hydrogen bonding brings some changes such as smaller wavenumbers on $-NO_2$ asymmetric stretching, >C═O stretching, and N−H stretching.

On the other hand, there are some vibrations that did not show a strong influence of hydrogen bonding on the same functional groups as $-NO_2$ and N−H.

Experimental IR bands at 1340 and 1355 cm^{-1} are assigned as combinations of $-NO_2$ symmetric stretching, $-NO_2$ deformation, N−H deformation, and ring deformation as listed in Table 3. The values of the gas phase (Ar matrix) for those vibrations are 1338 (mode 21) and 1361 cm^{-1} (mode 20). These differences (2 and 6 cm^{-1}) are smaller compared to the deviation of mode 23 $-NO_2$ asymmetric stretching with 22 cm^{-1}. This implies that there is a tendency of deformation to depend on the displacement vectors of the normal mode. In the case of $-NO_2$, symmetric motions (modes 20 and 21) couple together, but their moving area and change of electronic states may be smaller than those of asymmetric motion. This is due to the fact that hydrogen bonding has a stronger effect on the symmetric motion than on asymmetric motion.

A similar effect was observed on N−H deformations in plane, where the vibrations are coupled with ring motions. IR bands at 1006 and 1473 cm^{-1} are related to N−H deformations in plane. Those deviation values from the gas-phase wavenumbers are 15 and 10 cm^{-1}, respectively, while the N−H stretching wavenumber in the gas phase (3489 cm^{-1}) is about 300 cm^{-1} higher than that in the crystal (3198 cm^{-1}). The hydrogen bonding may affect only the direction of N−H bond axis (the same direction as the stretching mode), and this strong effect may cause the deformation of some ring vibrations.

4. Conclusions

The vibrational assignment of NTO was experimentally accomplished with stable isotope-labeled NTO compounds. Vibrational calculation of $-NO_2$ asymmetric stretching showed good agreement with the experimental data, and was completely determined in this work.

Theoretical assignment of vibrational bands was performed and most of the bands were assigned by using both experimental and theoretical data.

By using those results, the effects of hydrogen bonding in the crystalline state are apparent. Not only were there changes of bond lengths related to hydrogen atoms and oxygen atoms, but there were also some interesting ring deformations in the crystalline phase compared to the structure in the gas phase.

Acknowledgment. The authors greatly appreciate the help and the understanding of Professor Ko Saito of Hiroshima University and Professor Kazuyoshi Takayama of Tohoku University for our research. We also thank Okazaki National Research Institute of Molecular Science for the use of the Fujitsu VPP5000. Additionally, the authors appreciate the useful suggestions and devotional help of Dr. Bryce C. Tappan of Los Alamos National Laboratory.

References and Notes

(1) Williams, G. K.; Brill, T. B. *J. Phys. Chem*. **1995**, *99*, 12536−12539.

(2) Singh, G.; Kapoor, I. P. S.; Mannan, S. M.; Tiwari, S. K. *J. Hazard. Mater*. **1999**, *A68*, 155−178.

(3) Oxley, J. C.; Smith, J. L.; Rogers, E.; Dong, X. X. *J. Phys. Chem. A* **1997**, *101*, 3531−3536.

(4) Östmark, H.; Bergman, H.; Aqvist, G.; Langlet, A.; Persson, B. *Proc. 16th Int. Pyrotech. Semin.* **1991**, *16*, 874−886.

(5) Sanderson, A. J. NIMIC database, Sept 30, 1997.

(6) Piteau, M.; Becuwe, A.; Finck, B. *ADPA Symposium*, San Diego, CA, April 1991, pp 69−79.

(7) Becuwe, A.; Delclos, A. *Propellants Explos. Pyrotech.* **1993**, *18* (1), 1−10.

(8) Lee, K.-y.; Gilardi, R. *Mater. Res. Soc. Symp. Proc*. **1993**, *295*, 237−242.

(9) Bolotina, N. B.; Zhurova, E. A.; Pinkerton, A. A. *J. Appl. Crystallogr*. **2003**, *36*, 280−285.

(10) Zhurova, E. A.; Pinkerton, A. A. *Acta Crystallogr. B* **2001**, *B57*, 359−365.

(11) Ritchie, J. P. *J. Org. Chem*. **1989**, *54*, 3553−3560.

(12) Harris, N. J.; Lammertsma, K. *J. Am. Chem. Soc.* **1996**, *118*, 8048−8055.

(13) Sorescu, D. C.; Sutton, T. R. L.; Thompson, D. L.; Beardall, D.; Wight, C. A. *J. Mol. Struct.* **1996**, *384*, 87−99.

(14) Sorescu, D. C.; Thompson, D. L. *J. Phys. Chem. B* **1997**, *101*, 3605−3613.

(15) Meredith, C.; Russell, T. P.; Mowrey, R. C.; MacDonald, J. R. *J. Phys. Chem. A* **1998**, *102*, 471−477.

(16) Wang, Y. M.; Chen, C.; Lin, S. T. *THEOCHEM* **1999**, *460*, 79−102.

(17) Yim, W. L.; Liu, Z. F. *J. Am. Chem. Soc*. **2001**, *123*, 2243−2250.

(18) Kohno, Y.; Takahashi, O.; Saito, K. *Phys. Chem. Chem. Phys*. **2001**, *3*, 2742−2746.

(19) Oxley, J. C.; Smith, J. L.; Yeager, K. E. *J. Energy Mater*. **1995**, *13*, 93−105.

(20) Frisch, M. J.; Trucks, G. W.; Schlegel, H. B.; Scuseria, G. E.; Robb, M. A.; Cheeseman, J. R.; Zakrzewski, V. G.; Montgomery, J. A.; Stratmann, R. E., Jr.; Burant, J. C.; Dapprich, S.; Millam, J. M.; Daniels, A. D.; Kudin, K. N.; Strain, M. C.; Farkas, O.; Tomasi, J.; Barone, V.; Cossi, M.; Cammi, R.; Mennucci, B.; Pomelli, C.; Adamo, C.; Clifford, S.; Ochterski, J.; Petersson, G. A.; Ayala, P. Y.; Cui, Q.; Morokuma, K.; Salvador, P.; Dannenberg, J. J.; Malick, D. K.; Rabuck, A. D.; Raghavachari, K.; Foresman, J. B.; Cioslowski, J.; Ortiz, J. V.; Baboul, G.; Stefanov, B. B.; Liu, G.; Liashenko, A.; Piskorz, P.; Komaromi, I.; Gomperts, R.; Martin, R. L.; Fox, D. J.; Keith, T.; Al-Laham, M. A.; Peng, C. Y.; Nanayakkara, A.; Challacombe, M.; Gill, P. M. W.; Johnson, B. G.; Chen, W.; Wong, M. W.; Andres, J. L.; Gonzalez, C.; Head-Gordon, M.; Replogle, E. S.; Pople, J. A. *Gaussian 98*, revision A.11.1; Gaussian, Inc.: Pittsburgh, PA, 2001.

(21) Forseman, J. B.; Frisch, A. *In Exploring Chemistry with Electronic Structure Methods*; Gaussian, Inc.: Pittsburgh, PA, 1996.

(22) Franken, J.; Hambir, S. A.; Dlott, D. D. *J. Appl. Phys.* **1999**, *85* (4), 2068−2074.

(23) Prabhakaran, K. V.; Naidu, S. R.; Kurian, E. M. *Thermochim. Acta* **1994**, *241*, 199−212.